第27卷 第4期
2006年4月

半 导 体 学 报
CHINESE JOURNAL OF SEMICONDUCTORS

Vol. 27 No. 4
Apr. ,2006

An Open-Loop Test of a Resonator Fiber Optic Gyro *

Zhang Xulin, Ma Huilian†, Jin Zhonghe, and Ding Chun

(Department of Information Science & Electronic Engineering, Zhejiang University, Hangzhou 310027, China)

Abstract: The resonator fiber optic gyro (R-FOG), which utilizes a resonance frequency change due to the Sagnac effect, is a promising candidate for the next generation inertial rotation sensor. In this study, an open-loop R-FOG is set up using phase modulation spectroscopy. First, the demodulation curve is obtained using a lock-in amplifier. From the demodulation signal, a gyro dynamic range of ±4.2rad/s is obtained. Then, using different phase modulation frequencies, the open-loop gyro output signal is measured when the gyro is rotated clockwise or counterclockwise. The bias drift as a function of time is also measured. The fluctuation of the output over 5s is about 0.02rad/s. The drift can be reduced by taking countermeasures against system noise.

Key words: optoelectronics; resonator fiber optic gyro; phase modulation spectroscopy
EEACC: 4250; 7230E
CLC number: TN815 **Document code:** A **Article ID:** 0253-4177(2006)04-0688-04

1 Introduction

Fiber optic gyros based on the Sagnac effect[1] have recently been proposed and investigated, including the interferometer fiber optic gyro (I-FOG) and the resonator fiber optic gyro (R-FOG). The I-FOG has been used in navigational and other traditional applications. For guidance applications, a fiber coil longer than 1km is used. Such a long fiber increases gyro drift due to the time variant temperature distribution in the sensing coil, which inhibits the performance. The R-FOG is a frequency-sensitive device. An R-FOG with a fiber ring about 5~10m in length can achieve the same performance as an I-FOG with a 1km long fiber coil. R-FOGs have become appealing devices for many applications in navigation and guidance[2].

In this paper, an open-loop operation R-FOG system is presented. The signal detection is achieved by phase modulation (PM) spectroscopy[3] using $LiNbO_3$ phase modulators[4]. In PM spectroscopy, the modulating and feedback signals are separated, and the $LiNbO_3$ phase modulators are easily integrated with other optical devices, making the R-FOG system smaller[5].

2 Theory

Figure 1 shows a schematic diagram of the R-FOG used in this experiment. The resonator is the key sensing part in the R-FOG. It is composed of a 10m-long polarization-preserving fiber and a polarization-preserving fiber coupler with a coupling index of 10%. The diameter of the resonator is 0.1m, and the wavelength of the fiber laser (FL) is 1550nm, so the scale-factor of this system is 4.45×10^4 Hz/(rad/s)[1].

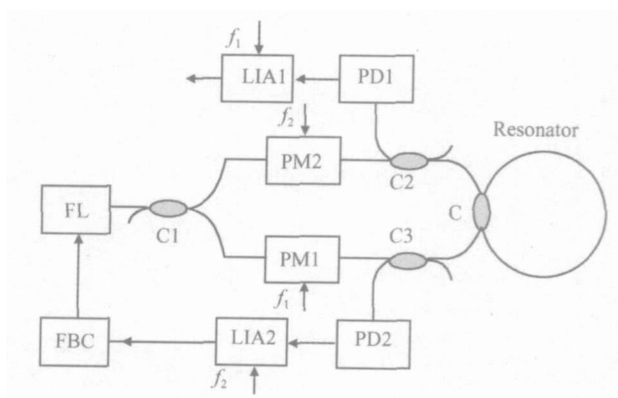

Fig. 1 Diagram of R-FOG using PM spectroscopy

The output light from the FL is split into two beams by the coupler C1. Each beam is sine wave

* Project supported by the Excellent Young Teachers Program of the MOE of China (No. 355 in 2003)

† Corresponding author. Email: mahl@zju.edu.cn

Received 12 November 2005, revised manuscript received 12 January 2006

phase modulated by the $LiNbO_3$ phase modulators PM1 and PM2 before being injected into the resonator. The two modulation frequencies f_1 and f_2 are set different to attenuate the backscattering noise[6].

The clockwise (CW) and counterclockwise (CCW) light waves in the resonator are sensed in reflection mode by photodiodes PD1 and PD2, respectively. The signals from PD1 and PD2 are demodulated in lock-in amplifiers LIA1 and LIA2. The output signals from LIA1 and LIA2 can be expressed as[3]

$$V_{out} = P \sum_n J_n(M) J_{n+1}(M) [h_n h_{n+1} \sin(\Phi_{n+1} - \Phi_n) - h_{-n} h_{-(n+1)} \sin(\Phi_{-n} - \Phi_{-(n+1)})] \quad (1)$$

where h_n is the amplitude of the resonator transmission function, Φ_n is the phase of the resonator transmission function, M is the modulation index, and P is a constant related to the system parameters. Equation (1) shows the relationship between the demodulation signal V_{out} and the resonance frequency deviation Δf[3]. Here, $\Delta f = f_{FL} - f_i$, where f_{FL} is the frequency of the FL, and f_i refers to the resonance frequency of the resonator. For CW light waves, $f_i = f_{CW}$, and for CCW light waves, $f_i = f_{CCW}$.

In accordance with Eq. (1), the relationship between V_{out} and Δf in the CW direction is shown in Fig. 2. Here, M and f_1 are set at 1 and 100kHz, respectively. There is a linear range from - 0.2 to 0.2MHz near the resonance point where Δf is 0, the amplitude of which is 3.9V. The scale-factor of this system is 4.45×10^4 Hz/(rad/s). The dynamic range of this system is ±4.5rad/s in theory. In the CCW direction, the demodulation curve from LIA2 is similar to that in Fig. 2. There is also a linear part near the resonance point. The feedback circuit (FBC) is used to lock f_{FL} at f_{CCW} using the slope of the linear part of the demodulation curve from LIA2. When the R-FOG is at rest, $f_{CW} = f_{CCW}$. While the R-FOG is rotating, there is a Sagnac frequency difference between f_{CW} and f_{CCW}, as shown in Fig. 3. According to the Sagnac effect[1], when the gyro is rotating in the CW direction, f_{CCW} is larger than f_{CW}. In this case, the gyro output from LIA1 is a positive voltage signal, as shown in Fig. 3. When the gyro is rotating in the CCW direction, the gyro output from LIA1 is a negative voltage signal.

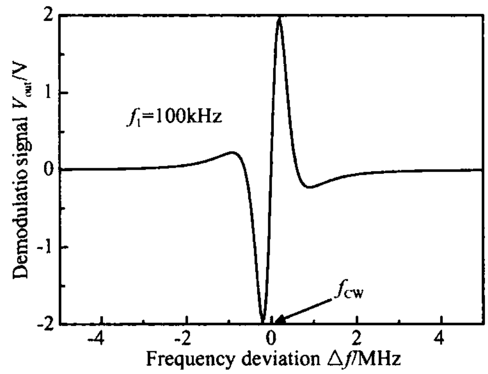

Fig. 2　Relationship between V_{out} and Δf

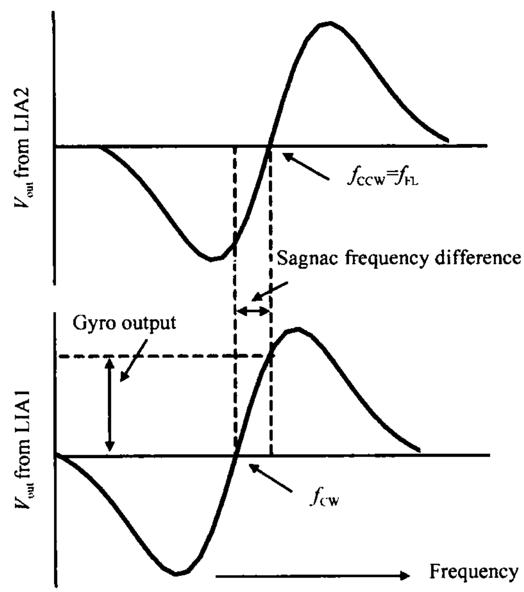

Fig. 3　Diagram of the gyro output signal　The R-FOG rotates in the CW direction.

3　Experiment and discussion

In the experiments, all system parameters are the same as the theoretical values in Fig. 2.

First, the resonance curve of the resonator is tested. A low frequency sawtooth-wave voltage is applied to the FL. The lasing frequency f_{FL} changes linearly with the time. The applied voltage is a sawtooth-wave with the amplitude of 120mV and the period of 20s. The oscilloscope trace in Fig. 4 shows the demodulation curve for CW direction. The amplitude and duration of the linear part of the demodulation curve are 3.625V and 250ms, respectively. Since f_{FL} changes linearly with the input voltage at 0.25GHz/V, f_{FL} changes linearly with the time at 1.5MHz/s by this sawtooth wave. This means that the linear part of the demodulation curve in Fig. 4 is ±0.188MHz. Since the scale-factor is 4.45 ×10^4 Hz/(rad/s), the dynamic range of this R-FOG is ±4.2rad/s. These experimental results are similar to the theoretical results in Fig. 2. Furthermore, the slope of the linear part in the demodulation signal from LIA1 is estimated from Fig. 4 to be 0.43V/(rad/s).

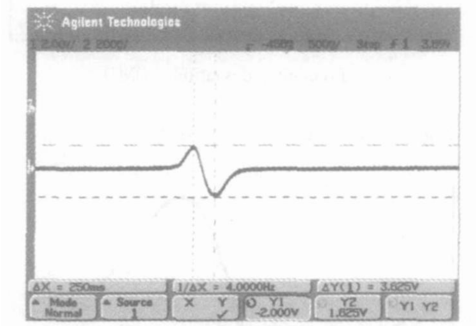

Fig. 4 Demodulation signal from LIA1

After obtaining the demodulation signal of the R-FOG, the open-loop system is set up. When f_{FL} is locked at f_{CCW}, the output signal from PD2 is stable, as shown in the lower curve in Fig. 5. When the resonator is rotating, the open-loop gyro output is observed from LIA1, as shown in the upper curve of Fig. 5. In the experiment, the rotation rate is increased to a certain value and then reduced to zero. Since the gyro output signal is proportional to the rotation rate, the gyro output signal changes with the rotation rate as shown in the upper curve of Fig. 5. The maximum value of the gyro output signal is 170mV. Because the slope of the linear part in the demodulation signal from Fig. 4 is 0.43V/(rad/s), the rotation is estimated to be about 0.4rad/s. From Fig. 5, when the resonator is rotating in the CW direction, the gyro output signal is a positive voltage, whereas when the resonator is rotating in the CCW direction, the gyro output signal is a negative voltage. This phenomenon is the same as Fig. 3 shows.

Finally, when the system is at rest, the drift of the R-FOG is tested. Figure 6 shows the drift of the R-FOG over 5s. The bias drift is approximately 10mV. This corresponds to a rotation rate of 0.02rad/s; but the shot-noise-limit of this system is 1.8 ×10^{-7} rad/s, theoretically[6]. The bias drift can be decreased by taking countermeasures against system noise, such as backscattering, polarization, and the Kerr effect[7].

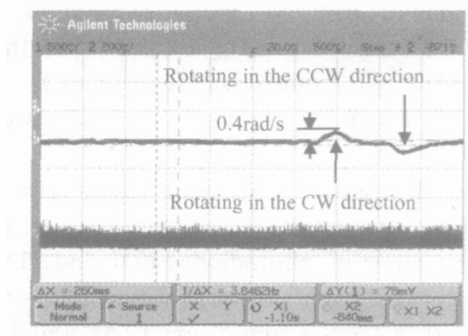

Fig. 5 Upper curve is the gyro signal from LIA1 when the R-FOG is rotating while the lower curve is the output signal from PD2.

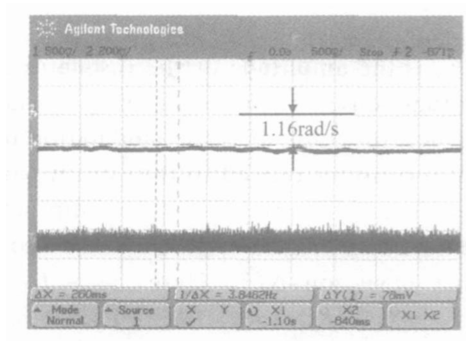

Fig. 6 Upper curve is the gyro signal from LIA1 when the R-FOG is at rest and the lower curve is the output signal from PD2.

4 Conclusion

In summary, an open-loop operation R-FOG system is set up with a phase modulation spectroscopy scheme using $LiNbO_3$ phase modulators. The open-loop gyro output is obtained. The bias drift as a function of time is also measured. The fluctuation of the output over 5s is about 0.02rad/s. In the future, the gyro sensitivity will be improved by noise suppression.

References

[1] Post E J. Sagnac effect. Rev Mod Phys, 1967, 39:475

[2] Carroll R, Coccoli C D, Cardarelli D, et al. The passive resonator fiber optic gyro and comparison to the interferometer fiber gyro. SPIE, 1986, 719:169

[3] Zhang Xulin, Ma Huilian, Ding Chun, et al. Analysis on phase modulation spectroscopy of resonator fiber optic gyro. Chinese Journal of Lasers, 2005, 32(11):1529 (in Chinese) [张旭琳, 马慧莲, 丁纯, 等. 谐振式光纤陀螺调相检测分析. 中国激光, 2005, 32(11):1529]

[4] Hotate K, Harumoto M. Resonator fiber optic gyro using digital serrodyne modulation. J Lightwave Technol, 1997, 15(3):466

[5] Suzuki K, Takiguchi K, Hotate K. Monolithically integrated resonator microoptic gyro on Silica planar lightwave circuit. IEEE J Lightwave Technol, 2000, 18(1):66
[6] Iwatsuki K, Hotate K, Higashiguchi M. Effect of Rayleigh backscattering in an optical passive ring-resonator gyro. Appl Opt, 1984, 23(21):3916
[7] Hotate K, Takiguchi K. Drift reduction in an optical passive ring-resonator gyro. SPIE, 1991, 1585:116

谐振式光纤陀螺开环响应测试 *

张旭琳 马慧莲† 金仲和 丁 纯

(浙江大学信息与电子工程系, 杭州 310027)

摘要: 谐振式光纤陀螺是基于光学 Sagnac 效应来测量载体旋转角速度的一种新型传感器. 利用调相谱检测技术, 建立了谐振式陀螺的开环响应测试系统. 利用自行研制的锁相放大器和反馈控制电路, 得到了线性度很好的解调曲线. 从解调曲线的线性工作区可进一步得到系统的动态范围高达 +4.2～-4.2rad/s. 通过对顺时针和逆时针光路采用不同的频率调制, 成功地观察到对应两个不同旋转方向的陀螺开环响应输出信号. 最后, 对系统的零漂进行了测试, 在 5s 时间内观察到系统的零漂为 0.02rad/s.

关键词: 光电子学; 谐振式光纤陀螺; 调相谱检测技术
EEACC: 4250; 7230E
中图分类号: TN815 **文献标识码**: A **文章编号**: 0253-4177(2006)04-0688-04

* 教育部优秀青年教师资助计划(批准号:教人司(2003)355号)
† 通信作者. Email: mahl@zju.edu.cn
2005-11-12 收到, 2006-01-12 定稿